ACS OMEGA

http://pubs.acs.org/journal/acsodf

Article

Lignosulfonates in Crude Oil Processing: Interactions with Asphaltenes at the Oil/Water Interface and Screening of Potential Applications

Sébastien Simon,* Marzieh Saadat, Jost Ruwoldt, Marcin Dudek, Ross J. Ellis, and Gisle Øye

Cite This: https://dx.doi.org/10.1021/acsomega.0c04654

Read Online

ACCESS | Metrics & More | Article Recommendations | Supporting Information

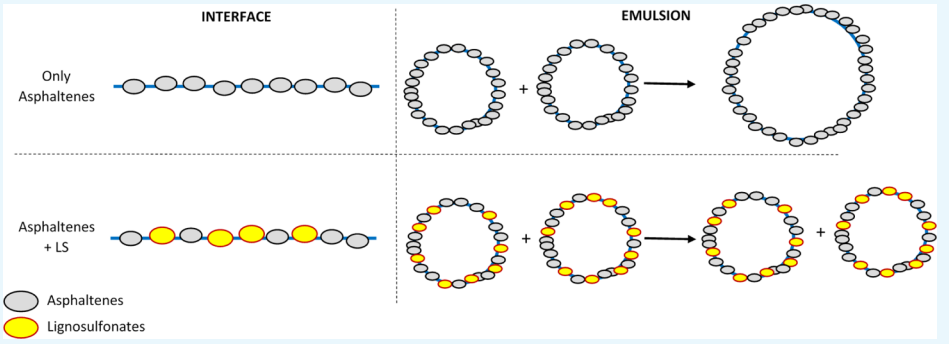

ABSTRACT: The goal of this article is to test the potential application of lignosulfonates (LSs) in crude oil production and processing. Three LS samples of varying hydrophobicity and average molecular weight were considered. First, the interfacial tension between brine and xylene and interfacial dilational rheology properties of LS samples were measured. It was found that the most surface-active LS sample has the lowest molecular weight in agreement with the results from the literature. In the presence of asphaltenes, all three LS samples were able to compete with asphaltenes, the most polar crude oil component, at the interface and form mixed LS−asphaltene interfaces. However, only the most surface-active LS sample among the three tested could fully desorb asphaltenes at the highest tested LS concentration (500 ppm). Second, three possible applications were screened. LSs were tested to prevent the formation of w/o crude oil emulsions or to break these. However, the opposite effect was observed, that is, stabilization of water-in-crude oil emulsions. The potential application of LS in produced water (PW) clarification was furthermore considered. The kinetics of PW clarification was found unaffected by the presence of LS, even at very high concentrations (1000 ppm). Finally, the potential of LS for enhanced oil recovery was assessed. The LS flood changed the surface wettability toward water wetness for one of the samples, yet LS injection did not recover additional oil beyond brine recovery. It was concluded that LS has interesting properties, such as the potential to compete with crude oil indigenous components at the oil/water interface. The stabilization action of LS was dominant over any destabilization effect, which led to the conclusion that LSs are more efficient for stabilizing emulsions rather than destabilizing.

1. INTRODUCTION

Lignosulfonates (LSs) are poly-branched anionic polymers, which are predominantly produced during sulphite pulping of wood. In contrast to other technical lignins, they generally exhibit good water solubility because of an abundance of sulfonate groups. As a result of condensation reactions during wood pulping, LS can exhibit a large range of molecular weight, that is, from 1000 to 150,000 g/mol,[1] and consequently a high polydispersity index.[2] Alternate methods have also been developed to modulate the chemical structure of LS especially in terms of degree of sulfonation, molecular weight, and functional groups.[3]

The presence of anionic groups and hydrophobic moieties, such as aromatic rings and aliphatic linkages, accounts for both hydrophilic and lipophilic properties of the LS. As a result, LS molecules can adsorb at binary interfaces. LSs have a different structure than classical surfactants. They are poly-branched polyelectrolyte macromolecules with multiple hydrophilic and hydrophobic moieties. This property makes LS attractive as dispersants in various industries.[4] For example, LSs are used as plasticizers in concrete, carbon black dispersants, dyestuff dispersants, and emulsion and suspoemulsion stabilizers.[3,5,6]

Received: September 22, 2020
Accepted: October 28, 2020

Despite the structural differences, LSs are affecting surface tension and interfacial properties in a similar manner as classical surfactants. At low concentration, a logarithmic dependence was found for surface or interfacial tension with LS concentration.[7−9] The compressibility of LS films at the water/oil interface depended strongly on pH and salinity.[10] LSs were shown to form viscoelastic interface layers, which were also greatly affected by the amount and type of added electrolytes.[11] Because of their hydrophilic character, LS-stabilized emulsions are usually of oil-in-water type.[12] Steric hindrance, electrostatic repulsion, and particle stabilization were mentioned as possible mechanisms for LS emulsion stabilization,[13,14] in addition to the formation of viscoelastic interfacial layers. Furthermore, it was shown that the stability of LS-stabilized o/w emulsions was a function of the LS hydrophobicity,[9] as determined by hydrophobic interaction chromatography. Higher hydrophobicity would impart higher emulsion stability, whereas lower average molecular weight tended to affect interfacial tension more strongly.

LS can adsorb onto solid surfaces such as dolomite, limestone, alumina, or titanium oxide.[15−18] The adsorption on solids was reported to follow the Langmuir isotherm.[19,20] Moreover, it was determined that the adsorbed amount increased with salt concentration because of reduced electrostatic repulsions.[16] However, this effect is more marked in the presence of $CaCl_2$ than with NaCl. By studying the adsorption of LS onto a dye with a quartz crystal microbalance (QCM), Qin et al.[21] also found that LS adsorption increases with ionic strength and decreases when the temperature is increased.

LS has been used for building self-assembly multilayers on the quartz surface with the polycation poly(diallyldimethylammonium chloride).[22−24] Analogous to LS self-association, this multilayer buildup was facilitated by high NaCl concentration. The authors concluded that the self-assembly behavior was governed by hydrophobic and π−cation interactions and not electrostatic interaction. LS interactions with chitosan have also been subject to research, as this is a biobased polycation. In an aqueous solution, LS and chitosan were reported to associate, forming insoluble complexes.[25] A technical application was proposed, in which LSs were removed from aqueous solutions via adsorption onto silica beads that had been cross-linked with chitosan.[20]

Interactions between LS and surfactants have also been studied. When LSs are mixed with an anionic surfactant such as sodium dodecylsulfate (SDS), the measured surface tensions are typical of a mixed surfactant system.[26] Complexation between LS and cationic surfactant was investigated by Askvik et al.[7,27] No beneficial effect on the creaming rates of oil-in-water emulsions was found; however, the authors concluded that a material could be produced, which had better oil solubility than the original surfactants. Qiu et al.[18] have shown that straight-chain alcohols can be used as a cosurfactant to improve the surface activity of LSs. Based on emulsion stability and the loss of compressive film stability, competitive interaction of LS and petroleum asphaltenes at the water/oil interface has been suggested.[10]

Considering the interesting interfacial properties of LS, its biodegradability, and the fact that it is produced from natural resources, LSs are viewed as an interesting alternative for several applications. For instance, extensive research has been conducted on utilizing LS as a sacrificial adsorbate for enhanced oil recovery (EOR).[28−31] LS-stabilized heavy oil-in-water emulsions for pipeline transport have been suggested,[32] as the emulsions would have lower viscosity than the heavy oil.

This article explores the possibility to expand the range of applications of LSs by considering their impact in crude oil production and processing. In this field, numerous surface-active chemicals are used to fulfill various tasks such as improving the separation between oil and water (demulsifiers and flocculants), treat produced water to remove oil droplets, or increase the amount of crude oil ultimately produced from oil field with the so-called EOR chemical-flooding operations.[33] The first part of the study will consider the interactions at the oil/water interface between LS and asphaltenes, that is, the crude oil components governing crude oil interface properties, to determine how the LS could affect crude oil interfacial properties. Then, three possible applications of LS in crude oil production and processing are considered:

- Separation of crude oil from water.
- Clarification of produced water.
- Use in EOR operations.

2. EXPERIMENTAL SECTION

2.1. Chemicals. Three lignosulfonate samples differing by their hydrophobicity and molecular weights were studied. These samples were previously used by Ruwoldt et al.[9] and are hence labeled with their corresponding alias. These samples are commercial sodium lignosulfonates that were prepared, purified, and analyzed by Borregaard AS. Their characteristics are summarized in Table 1.

Table 1. Hydrophobicity and Molecular Weights of Lignosulfonate Used in This Study

LS sample	$\overline{M_n}$ g/mol[a]	relative hydrophobicity[b]
LS-3	2700	0.24
LS-4	2800	0.44
LS-6	1800	0.54

[a]Determined by gel permeation chromatography. [b]Relative hydrophobicity calculated from the average elution peak determined by hydrophobic interaction chromatography (HIC). See Ruwoldt et al.[9] for the details of the calculation.

Two crude oils were used in this study named A and B. A is a conventional oil and B is a heavy crude oil. Some of their features are summarized in Table 2.

Asphaltenes were extracted by adding 40 mL of *n*-hexane for 1 g of crude oil B; the sample size was either 4 or 10 g depending on the needs. The mixture was then stirred overnight. The next day, the asphaltene fraction is recovered by vacuum filtration using a 0.45 μm HVLP (millipore) membrane filter. The filtrate is washed up with warm *n*-hexane and finally dried under a N_2 atmosphere.

The following chemicals were used without further purification: sodium dodecylsulfate (SDS, ≥ 99.0%, Sigma-Aldrich), 3-(*N*-morpholino)propanesulfonic acid (MOPS, ≥ 99.5%, Sigma-Aldrich), sodium chloride (for analysis, Merck), sodium hydroxide (≥99%, VWR), methyltrioctylammonium chloride (MTOAC, ≥ 97.0%, Sigma-Aldrich), xylene (mixture of isomers, ≥ 98.5%, VWR), and decane (≥99%, Sigma-Aldrich). Deionized water was from a Milli-Q system (Millipore).

https://dx.doi.org/10.1021/acsomega.0c04654
ACS Omega XXXX, XXX, XXX−XXX

Table 2. Physical and Chemical Properties of Crude Oils[a]

			SARA analysis			
crude oil	density at 25 °C, g/mL	viscosity at 25 °C, mPa·s	saturates (wt %)	aromatics (wt %)	resins (wt %)	asphaltenes, hexane insoluble (wt %)
A	0.879	15.0	74.6	19.7	5.3	0.35
B	0.932	218	37.4	44.1	16.1	2.45

[a]Characteristics of crude oil B are taken from Simon et al.[34] The SARA composition determination method by HPLC is described by Hannisdal et al.[35]

2.2. Solution Preparation. Stock buffer solutions containing 1160 mM NaCl and 40 mM MOPS were prepared, and their pH values were adjusted to 7 by adding aliquots of 1 M NaOH.

Stock aqueous LS solutions (1−5 wt %) were prepared by dissolving LS powder into Milli-Q water and shaking. They were then diluted by first adding Milli-Q water and then stock buffer solutions to the desired LS concentration in 580 mM NaCl and 20 mM MOPS. LS solutions (100 ppm) prepared this way were subsequently diluted with stock buffer solutions and Milli-Q water to reach the desired concentrations.

Asphaltene solutions were prepared at a concentration of 0.5 wt % by dissolving solid asphaltenes in xylene, then the mixture is sonicated for 10 min, and then shaken at 200 rpm overnight. The next day, the absence of flocs is confirmed by microscopy before sonicating the solutions for additional 10 min.

LSs were extracted and dissolved into an organic solvent (xylene) by complexation with quaternary ammonium using the following procedure: 100 mL of 20 g/L LS-6 in Milli-Q water and 100 mL of a solution of 80 g/L MTOAC in xylene are shaken overnight. Then, the two phases are fully separated by centrifugation (4000 rpm, 5 min). The aqueous and xylene phases are then, respectively, colorless and dark indicating that most of the LS-6 has been transferred into the organic phase. The organic phase was then pipetted and recovered.

2.3. Interfacial Tension and Interfacial Dilational Rheology Measurements. Interfacial tension and interfacial dilational rheology moduli were measured with a sessile/pendant drop tensiometer (PAT 1M) from SINTERFACE Technologies (Berlin, Germany) fitted with a hook.

Interfacial tension values were determined by recording the profile of the oil drop in the aqueous phase and fitting it with the Young−Laplace equation in the SINTERFACE PAT 1M v. 1.5.0.732 software. The interfacial dilational moduli E' (function of the elasticity of the interface) and E'' (function of the viscosity of the interface) were determined by sinusoidally varying the droplet volume. The complex dynamic apparent dilatational modulus (E^*) is defined as the Fourier transform ($\mathcal{F}$) of the change in interfacial tension (γ) relative to the change in the interfacial area of the droplet according to eq 1[36]

$$E^*(\omega) = \frac{\mathcal{F}\{\Delta\gamma(t)\}}{\mathcal{F}\{\Delta \ln(A(t))\}} = E'(\omega) + iE''(\omega) \quad (1)$$

with ω being the angular frequency of the oscillation.

A xylene droplet (15−45 μL, with or without asphaltenes) was created at the tip of the hook in a cuvette filled with 20 mL of aqueous phase (LS in NaCl 580 mM, MOPS 20 mM, and pH = 7). The droplet volume was kept constant for 1 h. During this time, interfacial tension at the interface between the xylene and the aqueous phase is continuously determined and recorded. After 1 h, oscillating measurements were performed to determine the E' and E'' moduli. The procedure consisted of five cycles of five different periods (100, 80, 60, 40, and 20 s) at a volume amplitude of 7% while keeping the same average volume as during the first hour. The amplitude had to be reduced to 2% for most of the LS-6 + asphaltene systems to obtain sinusoidal variations of the IFT with time. Only moduli obtained at a period of 100 s are reported.

2.4. Crude Oil Emulsion Preparations and Stabilities. Two procedures were carried out depending whether LSs were introduced before or after emulsification.

In the first case, 10 g of aqueous phase (LS in NaCl 580 mM, MOPS 20 mM, pH = 7) and 15 g of crude oil A are mixed at 1500 rpm (IKA Eurostar digital) with a four-blade propeller for 2 min. The formed emulsion is then transferred to a 100 mL graduated conical flask and the volume of free brine is visually determined and logged as a function of time for 1 h.

In the second case, 10 g of buffer solution (NaCl 580 mM, MOPS 20 mM, pH = 7) and 15 g of crude oil A are mixed at 2000 rpm (IKA Eurostar digital) with a four-blade propeller for 3 min. Then, 0.880 mL of xylene solution (containing either pure xylene, only MTOAC, or a mixture of MTOAC and LS-6, see Section 2.2) is introduced and manually shaken for 10 times. The formed emulsion is then transferred to a 100 mL graduated conical flask and the volume of free brine is visually determined and logged as a function of time for 1 h.

2.5. Turbidity Measurements for Assessing Produced Water Clarification. Oil-in-water emulsions (o/w) were prepared at an oil concentration of 500 ppm by introducing between 20.0 and 21.0 mg of crude oil and 40 g of NaCl 580 mM, MOPS 20 mM, pH = 7 buffered solution into 60 mL tubes. Mixtures were then stirred either at 10,000 or 18,200 rpm for 3 min with an Ultra-Turrax T-25 fitted with an S25N-10G dispersing tool (IKA) and ≈20 mL was then transferred into Turbiscan tubes. The transmittance and absorbance of samples were then scanned (2 scans in 1 min), before introducing 0.380 mL of LS-3 solution in NaCl 580 mM, MOPS 20 mM, pH = 7. A total of 14 extra scans were then performed in 13 min. The temperature was set at 25 °C.

To follow-up the clarification of the samples, the transmittance was averaged at the center of the tube (between 23 and 27 mm), and the difference with the initial averaged transmittance was calculated and reported.

2.6. Microfluidic Study of Oil Recovery. A microfluidic setup consisting of a syringe pump (Chemyx—Fusion 4000), camera (Canon 90D), and microfluidic device (Micronit Microtechnologies) was used for assessing the EOR capabilities of the LS samples, LS-3 and LS-6. The setup and procedure were developed in a previous study.[37] The micromodel is made of borosilicate glass through isotropic etching and consists of a uniform network of channels as well as inlet and outlet channels for even introduction and collection of the fluids.[38,39]

Two types of tests were performed using the setup: one-step recovery and two-step recovery (later named EOR) tests. One-step recovery tests include saturation of the chip with crude oil

https://dx.doi.org/10.1021/acsomega.0c04654
ACS Omega XXXX, XXX, XXX−XXX

B, aging for 1 h under ambient conditions, and injection of 10 μL of NaCl 580 mM, MOPS 20 mM, pH = 7 solution or LS-3 or LS-6 solutions (100 ppm in the same medium) at 0.5 μL/min. The EOR tests include saturation of the chip with crude oil B, aging for 1 h under ambient conditions, injection of 10 μL of high salinity brine (600 mM NaCl) at 0.5 μL/min as the secondary stage or improved oil recovery (IOR), and injection of 10 μL of LS-3 (100 ppm in NaCl 580 mM, MOPS 20 mM, pH = 7) at 0.5 μL/min. A combination of a microscope (Nikon ECLIPSE Ti2-U) and camera (Photron FASTCAM Mini WX100) was also used to investigate the extent of wettability alteration after different floodings. All steps were performed at room temperature (22 °C). Each test was repeated three times.

The images taken during the processes are then processed and analyzed based on the change in oil saturation to calculate the recovery factor (RF), the ratio of the extracted oil to the original oil in place.

3. RESULTS AND DISCUSSION

3.1. Interfacial Properties of Lignosulfonates and Competitive Adsorption between LS and Asphaltenes.

3.1.1. Interfacial Properties of LSs. The first part of this study was to analyze the interfacial properties of LS samples and their interactions at the interfaces with asphaltenes. The latter are one the most important components in crude oil that are responsible for interfacial properties and the stability of crude oil emulsions.[40,41]

Figure 1 presents the variations with time of the interfacial tensions at the brine/xylene interface in the presence of various

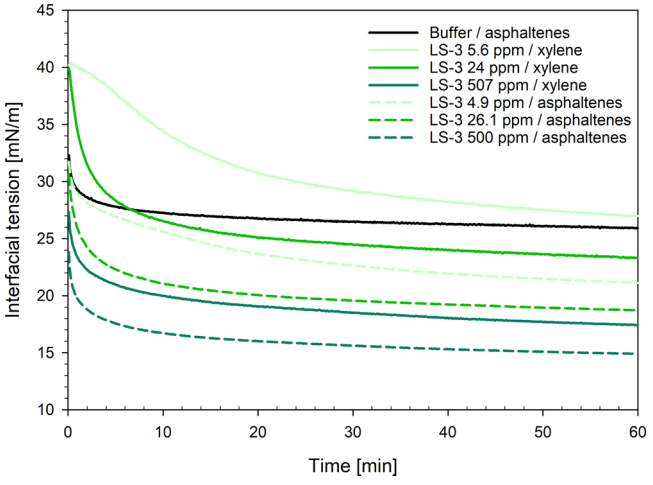

Figure 1. Kinetics of adsorption at the liquid/liquid interface of only asphaltenes, only lignosulfonate LS-3 and mixtures of lignosulfonate LS-3 and asphaltenes (0.5 wt %). Two parallels per systems were performed.

concentrations of LS-3 (from 4.9 to 507 ppm). The obtained curves are typical of the surfactant with a decrease in the IFT when the time increases,[42−44] indicating adsorption of LS-3 at the interface. No IFT plateau is reached after 1 h, especially at low LS concentration. The slow kinetics is most likely related to the polydispersity in molecular weight and composition of LS samples which induces competitive adsorption between the different LS molecules. A discussion of the kinetics of interfacial lignosulfonate adsorption has been given in a previous report.[11]

Figure 2 compares the variations of the IFT after 1 h of adsorption for the three LS systems investigated. It can be

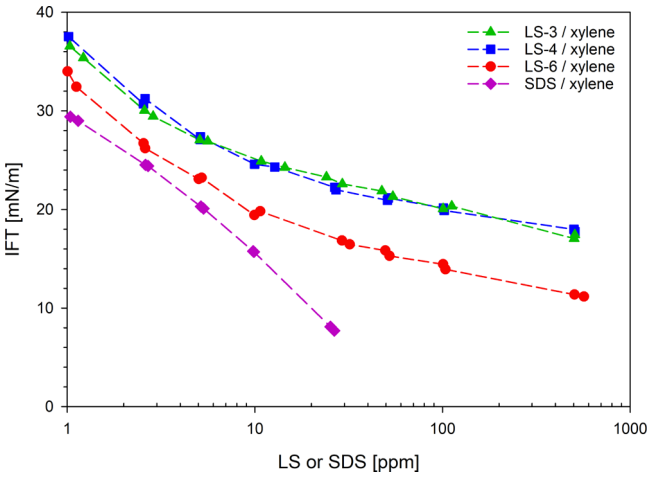

Figure 2. Variations of the interfacial tension with lignosulfonate concentration for the three LS samples at the liquid/liquid interface after 1 h of adsorption. No asphaltene is present in the studied systems. Data for SDS are also presented for comparison. The lines are guides for eyes.

noticed that the IFT values reported in the curves are not actual equilibrium values because no IFT plateau is reached after 1 h of adsorption (especially at the lowest concentrations tested); however, the reported values allow us to compare the LS systems with each other. The variations of the IFT with concentrations are similar for the 3 LS samples. They all are surface-active from low ppm concentration. LS-3 and LS-4 present the same surface activity despite their differences in molecular weight and hydrophobicity. LS-6 is significantly more surface-active than the two other LS products, which is, among other reasons, likely caused by its lower molecular weight. These results are consistent with data obtained on the same products studied with a spinning drop tensiometer.[9]

Extra information on the adsorption of LS at the oil/brine interface can be obtained by interfacial dilational rheology. Figure 3a compares the interfacial rheology moduli E' for the three LS samples. The E'' moduli are not presented because they are systematically lower than their respective E' moduli showing the predominant elastic character of LS samples at the interface. All the curves presented in Figure 3a show a maximum of E' when the concentration of LS is varied. In addition, E' increases in the order LS-3 < LS-4 < LS-6. The interpretation of interfacial dilational rheology data is generally not straightforward. Indeed, even if there is "rheology" in the name of the technique, the moduli E' and E'' measured using this technique only partially depend on "true" interfacial rheology properties. As a general rule, E' and E'' depend on:

- Interfacial rheology per se.
- Adsorption/desorption of the surfactants to and from the interface.

In the case of "classical" surfactants at the interface, such as Span 80,[42,45] it is mostly the adsorption/desorption that dominates the response, and interfacial rheology data can be analyzed using the Lucassen−van den Tempel model.[46] In the case of interacting complex systems such as protein[47] or ARN tetrameric acid/Ca^{2+}[48] that can form gel at the interface, E' and E'' mostly represent the rheology of the interface. In the

https://dx.doi.org/10.1021/acsomega.0c04654
ACS Omega XXXX, XXX, XXX−XXX

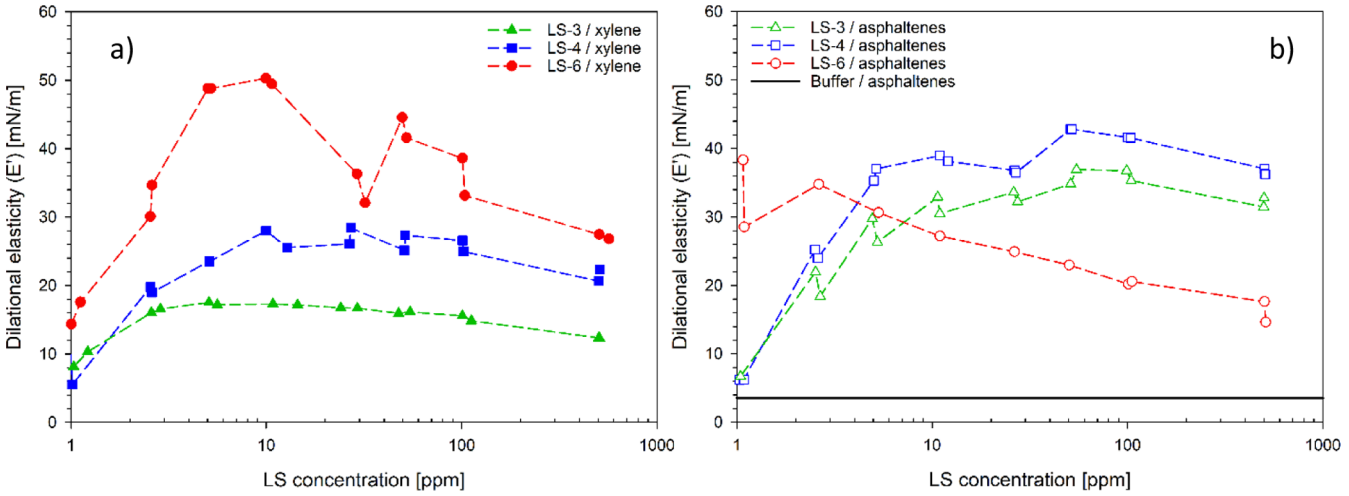

Figure 3. Variations of E' (measured at a period of 100 s) with lignosulfonate concentration measured after 1 h of adsorption: (a) in the absence of asphaltenes; (b) in the presence of 0.5 wt % asphaltenes. The lines are guides for eyes.

specific case of LS, it can be noticed that, even if LS-3 and LS-4 display similar IFT values, their E' is significantly different. Consequently, layers covered with LS-3 and LS-4 have different internal dynamic, that is, different rates of exchange of molecules between the layer and the bulk phases on one side and/or different interfacial elasticity and viscosity on the other side.

In order to evaluate the ability of LSs as surfactants, they were compared with a classical low-molecular-weight surfactant sodium dodecylsulfate (SDS) because LS and SDS are both anionic (Figure 2). The figure shows that the decrease in IFT is higher in the presence of SDS than LS at the same mass concentration, indicating that the SDS is more efficient to lower interfacial tension. However, if the same data are replotted as a function of the molar concentration (using the number average molecular weight for LS, Figure S1), the differences are less marked, and it can be noticed that the reduction of IFT happens for similar molar concentration ranges for both SDS and LS. Finally, it can also be noticed from Figure S1 that the IFT decrease with molar concentration is steeper in the cases of SDS compared with LS. According to the Gibbs adsorption isotherm equation (eq 2), that means that the SDS surface excess is higher than for LS samples.

$$\Gamma = -\frac{1}{nRT}\cdot\frac{\mathrm{dIFT}}{\mathrm{dLn}(C)} \qquad (2)$$

with Γ being the surface excess, R being the ideal gas constant, n is a constant depending on the number of species adsorbing at the interface, and T being the temperature.

Finally, the influence of chemical nature of the oil phase on adsorption of LS at the oil/water interface was investigated. Two organic solvents were compared: decane and xylene (Figure 4). IFT values measured between LS-3 solution and decane are systematically higher than with xylene as an organic solvent. This trend is mostly attributed to the difference of internal cohesive forces between decane and xylene because the two sets of data are nearly superimposed if the difference of interfacial tension between the two oil phases and brine in the absence of LS is considered (14 mN/m). Despite the possibility of $\pi-\pi$ interactions between xylene and aromatic rings of LS, the adsorption of LS-3 at the interface between oil and the two organic solvents is therefore similar.

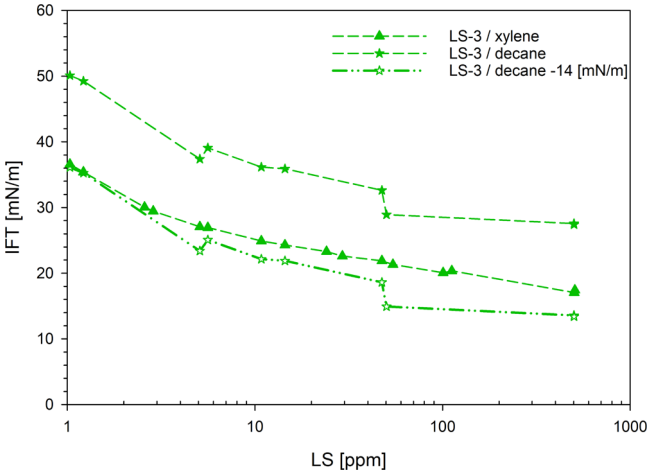

Figure 4. Comparison of the interfacial tension of lignosulfonate LS-3 measured at the decane or xylene/aqueous phase interfaces. The empty symbols correspond to the values measured in decane subtracted by 14 mN/m. The lines are guides for eyes.

3.1.2. Competitive Adsorption between LS and Asphaltenes. Asphaltenes are one of the most surface-active crude oil indigenous components.[49−51] They adsorb at the oil/water interface and stabilize crude oil emulsions. They also dominate the adsorption of crude oil on solid surfaces, thereby controlling their wettability.[52] Understanding how LSs could compete with asphaltenes to adsorb at the water/oil interface and interact would help to pinpoint possible applications of LS in crude oil production and processing.

First, information about the adsorption dynamics of asphaltenes together with LS systems can be obtained by analyzing the variations of the interfacial tension with time. These variations are presented in Figure 1 for LS-3 at various concentrations (already presented in Section 3.1.1), asphaltenes at a concentration of 0.5 wt %, and mixtures of asphaltenes and LS-3. It must be noticed that, due to their respective solubilities, LS-3 is initially present in the aqueous phase while asphaltenes are dissolved in xylene.

When asphaltenes are the only surface-active component present in the system, the interfacial tension quickly decreases to approximately 31 mN/m within 10 s. Then, the IFT

https://dx.doi.org/10.1021/acsomega.0c04654
ACS Omega XXXX, XXX, XXX−XXX

continues to decrease but at a lower rate. A value of 25.7 mN/m is reached after 1 h of adsorption. The kinetics of adsorption of asphaltenes at the oil/water interface has been recently explained by Schuler et al.[53]

When asphaltenes and LS-3 are both present, the IFT swiftly decreases to approximately 31−30 mN/m within 10 s at low LS-3 concentrations (4.9 and 26.9 ppm, respectively). Then, IFT continues to decrease during the next 1 h. The shape of the IFT reduction during this time is similar to the variations of the IFT with time for systems containing only LS-3. Therefore, it can be deduced that asphaltenes adsorb first and then LS-3 coadsorbs with asphaltenes at the interface. This order is perhaps related to the respective concentrations of both components. Indeed, the asphaltene concentration was chosen to be representative of asphaltene content in crude oil (Table 2), while LS concentrations are typical of demulsifier concentration used in crude oil processing. Hence, asphaltene concentration is several orders of magnitude higher than the LS concentration. This order explains why asphaltenes adsorb first because the adsorption rate and the IFT decrease are proportional to the bulk solute concentration during the initial moment of adsorption according to the Ward and Tordai equation.[43]

At the highest tested LS-3 concentration (500 ppm) and still in the presence of asphaltenes, the IFT has decreased to 22−23 mN/m after 10 s of adsorption and then continues to approach the system containing only LS-3 at the same concentration. Consequently, at such high LS concentration, asphaltenes and LS-3 coadsorb at short times. At longer times, only LS-3 continues to adsorb at the interface.

These conclusions are also valid for LS-4 (Figure S2) and mostly in the case of LS-6. The latter fully prevents adsorption of asphaltenes at high LS concentration (Figure S3) as explained in the following paragraphs.

Even if working with model systems allows us to obtain valuable information, some features of real systems are not reproduced such as the oil viscosity that should influence the bulk diffusion of asphaltenes and potentially their rate of adsorption.

The three LS systems are then compared by plotting the interfacial tension measured after 1 h of adsorption, with and without 0.5 wt % of asphaltenes (Figure 5). LS-6 systems are analyzed first because it is the most surface-active among the LS samples. The IFT of the LS-6 solution at the lowest tested concentration (≈1 ppm) in the presence of asphaltenes is close to the value for pure asphaltene solution but slightly lower. The IFT of the LS-6 solution at the lowest tested concentration (≈1 ppm) in the presence of asphaltenes is close to the value of the pure asphaltene solution but slightly lower. This means that asphaltenes are preponderant at the interface with a minor presence of LS-6. The incorporation of LS-6 at the interface at low LS concentrations when the IFT of LS-6 is higher than asphaltenes could be explained using the Langmuir equation for two-component systems. This equation, valid for noninteracting species, is the following for the adsorption of two components A and B[54]

$$\mathrm{IFT} = \mathrm{IFT}_0 - RT\Gamma_m \mathrm{Ln}(1 + K_{L,A}\cdot C_A + K_{L,B}\cdot C_B) \quad (3)$$

with Γ_m being the maximum adsorbed amount, IFT_0 being the interfacial tension of pure solvents, and $K_{L,A}$ and C_A being the Langmuir equilibrium adsorption constant and concentration of component A, respectively. This equation shows that IFT is lower when two components are present instead of one.

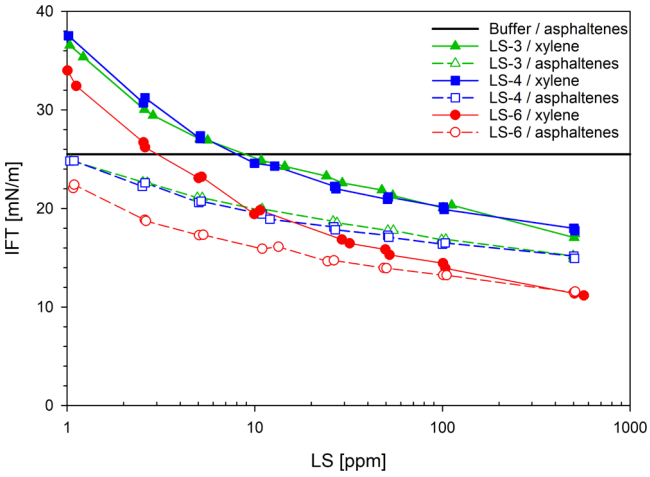

Figure 5. Variations of the interfacial tension with lignosulfonate concentration at the liquid/liquid interface with and without asphaltenes (0.5 wt %) measured after 1 h of adsorption. The horizontal line corresponds to the value measured in the presence of 0.5 wt % asphaltenes but in the absence of lignosulfonate. Other lines are guides for eyes.

When LS-6 concentration is increased, the IFT of mixed LS-6/asphaltene systems departs further and further from the value of pure asphaltenes showing that more and more LS-6 is adsorbed. However, these values are still lower than in the case of systems containing only LS-6 indicating that asphaltenes are still present in significant amount at the interface. In the presence of 500 ppm of LS-6, IFT data indicate that asphaltenes are no longer present at interfaces because the IFTs are identical with and without asphaltenes: LS-6 prevents adsorption of asphaltenes and desorbs already adsorbed asphaltene compounds.

The data for LS-3 and LS-4 in the presence of asphaltenes are similar. This is consistent with the fact that they display a similar interfacial behavior in the absence of asphaltenes despite their different molecular weights and hydrophobicities (Section 3.1.1). The variations of IFT with LS-3 or LS-4 concentrations in the presence of asphaltenes are similar to that of LS-6 with a predominant adsorption of asphaltenes at low LS concentration (few ppm) and then increasing LS adsorption at the interface when LS concentration increased. However, even at the highest tested LS-3 or LS-4 concentration, these two LS samples do not fully prevent adsorption of asphaltenes because IFT of asphaltenes−LS systems is lower than the values displayed by LS-3 and LS-4 in the absence of asphaltenes. This is consistent with the ranking of LS surface activity established in Section 3.1.1.

Figure 3b presents the interfacial dilatational modulus E' for the three LS systems in the presence of 0.5 wt % asphaltenes as a function of LS concentration. The E' value for the system containing only asphaltenes is also presented for comparison. The shape of the variations of the E' modulus with LS concentration is different between the LS-6-asphaltene system and the two other systems, meaning the dynamic properties of the adsorbed layers are different. It can also be noted that even at the highest tested LS-6 concentration (500 ppm), E' in the presence of asphaltenes is different from the modulus in the absence of asphaltenes, indicating the presence of asphaltenes in the absorbed layer, which is inconsistent with IFT data. A possible explanation could be that asphaltene concentration in the adsorbed layer would be too low to influence the IFT value

https://dx.doi.org/10.1021/acsomega.0c04654
ACS Omega XXXX, XXX, XXX−XXX

but enough to affect the E' modulus from the pure LS-6 layer. Concerning the LS-3 and LS-4 systems, the E' moduli in the presence of asphaltenes are different from pure LS systems which is consistent with the presence of a mixed LS−asphaltene layers, even at the highest LS concentrations (500 ppm), in consistence with IFT data. However, the E' values of the two LS−asphaltene systems are different, even if their IFT is the same. Consequently, even if the adsorbed amount must be similar, the dynamic of the interfacial layers is not, which is similar to the behavior of the LS-3 and LS-4 adsorbed layers in the absence of asphaltenes, as shown in Section 3.1.1.

The results presented above are consistent with results obtained using the Langmuir balance by Gundersen et al.[10] Indeed, these authors showed that LS and asphaltenes formed mixed films at the oil/water interface.

In conclusion, IFT and interfacial rheology measurements have allowed us to show that LSs are able to successfully compete with asphaltenes at the oil/water interface especially for the most surface-active LS sample (LS-6) at the highest tested concentration (500 ppm).

3.2. Assessment of Lignosulfonate as a Crude Oil Emulsion Inhibitor/Demuslifier. *3.2.1. Lignosulfonate Solubilized in the Aqueous Phase.* After studying the interfacial properties of 3 LS samples and their competitive adsorption with asphaltenes, some potential applications of LS in crude oil processing was evident and screening experiments were consequently conducted. First, it is discussed if LS could be used to help separate crude oil and water coproduced with it. As LS samples are only water-soluble, they cannot be directly added once water-in-crude oil emulsions are formed because LS would not be properly dispersed which should limit their efficiency. Consequently, LSs were introduced into the aqueous phase before the emulsions were created to determine if they could act as an inhibitor, that is, reduce the stability of crude oil emulsions and increase the oil/water separation rate.

Figure 6 presents the kinetics of free brine released for emulsions prepared from crude oil A in the presence of various concentrations of lignosulfonate LS-6 (from 0 to 100 ppm). In the absence of LS-6, good separation (80−90% free brine released) is reached in 20−30 min. If 11.5 ppm of LS-6 is present in the aqueous phase, the separation rate is not significantly modified considering the uncertainties in the measurement. On the contrary, at higher LS-6 concentration (100 ppm), there is nearly no free brine separated 60 min after emulsion preparation. This increase in stability is not due to an inversion phenomenon because the emulsion with 100 ppm of LS-6 is of w/o emulsion type as shown by conductivity measurement. Considering the IFT results presented in Section 3.1.2, it can be suggested that LS-6 will coadsorb with crude oil components (primarily asphaltenes) at the oil/water interface created during emulsification. This interfacial mixture will stabilize emulsions more efficiently than if the interface was only covered by crude oil components. This property is therefore opposite to the desired effect of crude oil emulsion inhibitors.

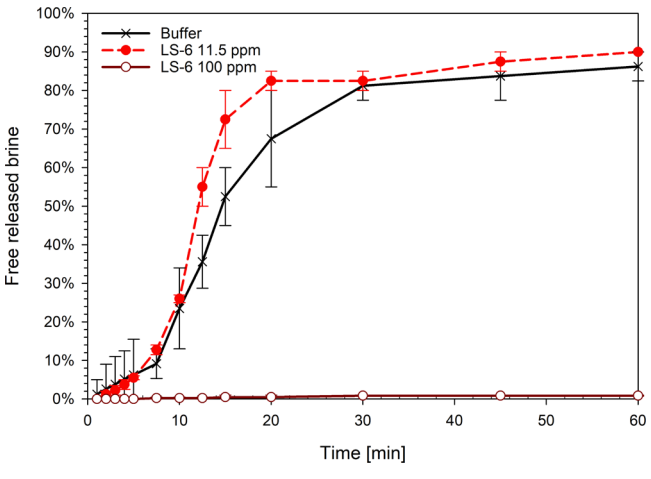

Figure 6. Bottle test showing the variations of the free water released with time for emulsions prepared from crude oil A in the presence of various concentrations of lignosulfonate LS-6. The indicated concentrations are calculated based on the mass of the aqueous phase. The values are averages of, respectively, 4 (no LS), 2 (11.5 ppm LS-6), and 2 (100 ppm LS-6) independent measurements. The error bars represent the range of values obtained and the lines are guides for eyes.

Similar bottle tests were performed with various concentrations of another LS sample: LS-4 (Figure 7). The trends are similar as in the presence of LS-6. Indeed, the stability of emulsions does not vary in the presence of 12 ppm of LS-4. Furthermore, the emulsions are more stable (less free brine released) at higher LS-4 concentrations (100 and 509 ppm). Here, also, this increase in stability is not due to an inversion phenomenon as shown by conductivity measurements performed on the emulsions prepared at the highest tested LS-4 concentration. Consequently, incorporation of LS-4 into the crude oil/brine interface increases the stability of crude oil emulsions toward coalescence.

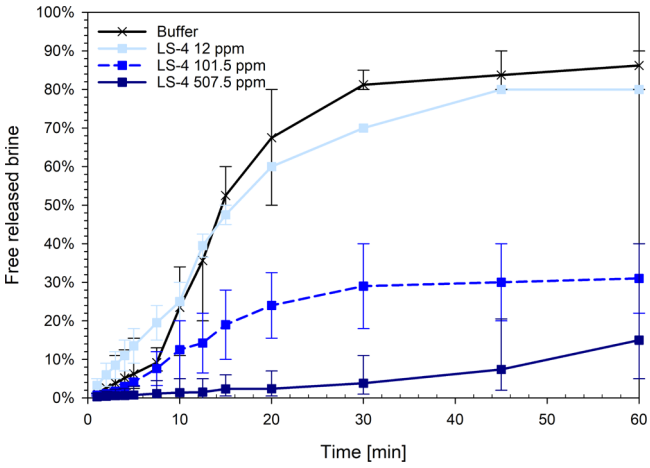

Figure 7. Bottle test showing the variations of the free water released with time for emulsions prepared from crude oil A in the presence of various concentrations of lignosulfonate LS-4. The indicated concentrations are calculated based on the mass of the aqueous phase. The values are averages of, respectively, 4 (no LS), 2 (12 ppm LS-4), 2 (100−103 ppm LS-4), and 4 (506−509 ppm LS-4) independent measurements. The error bars represent the range of values obtained and the lines are guides for eyes.

3.2.2. Lignosulfonate Solubilized in an Organic Solvent. One way to make LS oil soluble is by using a complexing agent, in this case, the quaternary ammonium methyltrioctylammonium chloride-MTOAC, which will transfer the LS into the organic phase (xylene). Authors have previously used long-chain aliphatic amines for the fractionation of lignosulfonates, based on this, the procedure in Section 2.2 was developed.[55] In

https://dx.doi.org/10.1021/acsomega.0c04654
ACS Omega XXXX, XXX, XXX−XXX

this way, LS-6 could be directly introduced into crude oil emulsions to determine its efficiency as a demulsifier. The procedure was not optimized, especially the concentration of MTOAC, as the goal was to screen possible LS applications.

Figure 8 presents the kinetics of free brine released for emulsions prepared from crude oil A after introduction of pure

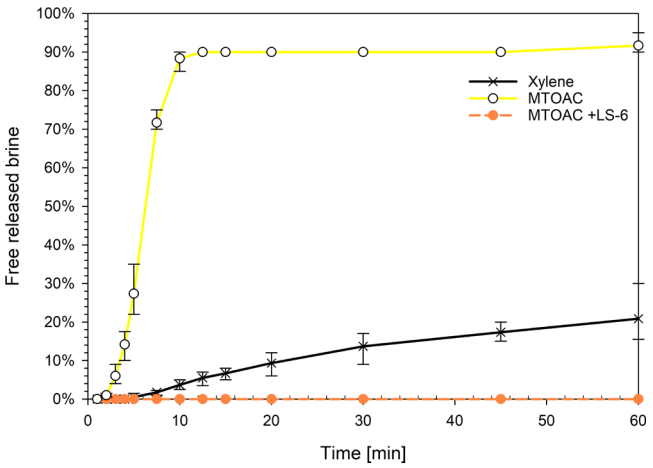

Figure 8. Bottle test showing the variations of the free water released with time for emulsions prepared from crude oil A and subsequent addition of pure xylene, MTOAC in xylene, and mixture of lignosulfonate and MTOAC in xylene. Concentrations added after emulsion preparation are 700 ppm LS-6 and 2800 ppm MTOAC (concentrations based on the emulsion masses). The values are averages of 3 independent measurements. The error bars represent the range of values obtained and the lines are guides for eyes.

xylene, MTOAC in xylene, and complex LS-6−MTOAC in xylene. If xylene is introduced (blank), the separation is incomplete 1 h after emulsion preparation with 21% free brine released. If MTOAC is introduced after emulsion preparation, good oil/water separation (80−90% free brine released) is reached in approximately 10 min indicating that MTOAC destabilizes crude oil emulsion. MTOAC is soluble and present in the organic phase, and once introduced in the crude oil emulsion sample, MTOAC could adsorb at the interface competing with the crude oil interfacial component and reduce the stability of w/o emulsions. Finally, if the MTOAC—LS-6 complex is introduced, emulsion stability strongly increases with no free water released 60 min after emulsion preparation. The emulsion is still of w/o type as shown by its conductivity. This means that the LS-6 or LS-6—MTOAC complex would adsorb onto the already formed crude oil/brine interface and prevent or limit coalescence between water droplets, which is detrimental for a possible demulsifier.

It must be noticed that while the pH is well-controlled during the introduction of pure xylene to crude oil emulsion (pH of the free brine released = 6.84), there is a significant decrease when MTOAC is introduced (5.9). It was not possible to determine the pH of the aqueous phase after introduction of LS-6 and MTOAC because no free brine was released. The pH variation could have an influence on the conclusions of this study because crude oil IFT and emulsion stability depend on pH.[50,56] The LS properties, especially the aggregation behavior, are also influenced by pH because of the variations of ionization degree of sulfonic, carboxyl, and phenolic groups.[57]

3.3. Assessment of Lignosulfonate to Treat Produced Water. Another possible application of LS in crude oil processing would be their implementation in produced water (PW) treatment. Produced water is the aqueous phase coproduced with oil. After oil/water separation, PW needs to be purified to meet regulation requirements before being discharged or reinjected.[58,59] In order to test if LS could be used to purify PW, model o/w emulsions were prepared, after which the kinetics of PW clarification was tested using the Turbiscan apparatus. This apparatus allows us to measure the transmittance and backscattering of samples as a function of time and height of the tube. Measurements showed that the transmittance of the samples increased with time which was attributed to the clarification of the samples by coalescence, flocculation, or creaming of oil droplets. Consequently, PW clarification was characterized by following the transmittance of PW samples measured at the center of the sample with time (Figure 9) after the addition of pure buffer (blank) or LS-3

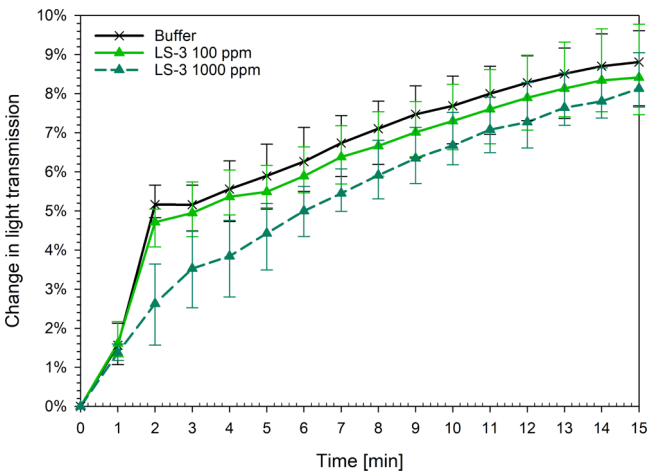

Figure 9. Evolution of the transmittance measured at the center of the samples. The samples were prepared by mixing 500 ppm of crude oil A with the aqueous phase at 10 000 rpm for 3 min. The lignosulfonate (LS-3) or a pure buffer is added after the second point is measured. The indicated concentrations correspond to the values after addition. The values are averages of, respectively, 4 (no LS), 3 (100 ppm LS-3), and 3 (1000 ppm LS-3) independent measurements. The error bars represent the range of values obtained and the lines are guides for eyes. One experiment performed by adding pure buffer was discarded: the initial transmittance was much lower than for the other tests.

solutions. The accuracy of the measurements required to perform several parallels can be estimated from Figure 9 to be 2−3% (in absolute values). Considering these uncertainties, the kinetics of clarification are similar if pure brine and 100 ppm of LS-3 are introduced in the PW samples. If more LS-3 is introduced (1000 ppm), it seems that the kinetics of clarification is slightly slower at short times, but similar final transmittances are reached after 900 s of clarification. Consequently, it appears that, even if injected at high concentration (1000 ppm), LS-3 has minor influence on the clarification of PW.

Other tests were performed by varying initial oil droplet size (Figure S4) and chemical nature of the crude oil (Figure S5). The results are similar.

3.4. Assessment of Lignosulfonate in EOR Applications. EOR designs all the methods which are aimed to recover more crude oil from a field by modifying physical and/

https://dx.doi.org/10.1021/acsomega.0c04654
ACS Omega XXXX, XXX, XXX−XXX

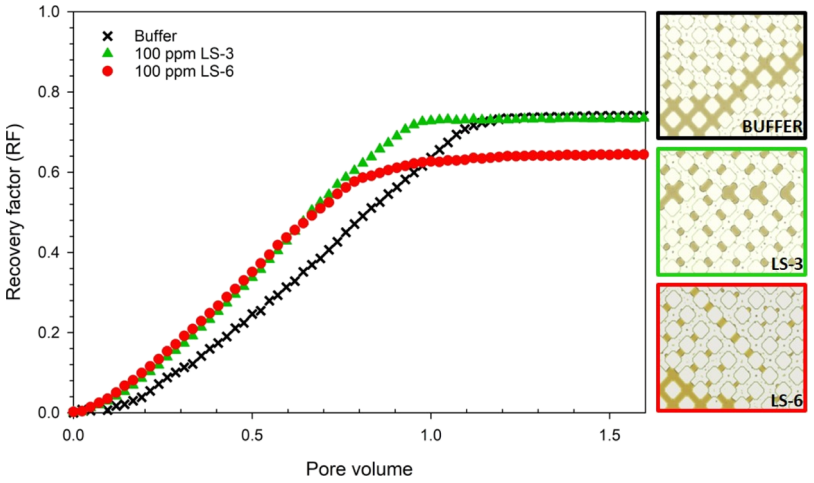

Figure 10. Recovery factor for crude oil B based on injected pore volumes of the NaCl-buffer solution, LS-3, and LS-6 (100 ppm). The micrographs of oil-flood arrangements after the one-step recovery tests with the three solutions are presented on the right. The color differences are because of different camera settings.

or chemical properties of reservoir rocks and/or fluids. Among these methods, surfactant flooding consists to inject surfactant solutions to decrease the interfacial tension between oil and water.[60] This ability is here tested with lignosulfonate.

3.4.1. One-Step Recovery Tests. During the one-step recovery tests, crude oil B was displaced with two LS floods. An additional test was conducted using NaCl 580 mM + buffer 20 mM solution for comparison. The average recovery factor for the three experiments versus injected pore volumes of the different floods is presented in Figure 10.

Based on these results, LS-3 was proved to be as effective as the NaCl-buffer solution in terms of RF. LS-3 reached the end of the network area (breakthrough) in a shorter amount of time. However, both experiments reached the same plateau after the breakthrough. LS-6 has the same recovery dynamic as LS-3 until breakthrough. The breakthrough happens earlier for LS-6 and, therefore, results in a lower recovery efficiency. LS-6 was also slower to reach plateau after breakthrough. The average breakthrough times (from when the flood reaches the network until breakthrough) for LS-3, LS-6, and NaCl-buffer solution were 220, 184, and 244 s, respectively. All three floods have similar displacement patterns and accomplish recovery through unstable displacement where viscous fingering happens. In order to assess the extent of wettability alteration induced by different flood types, the arrangement of the oil and aqueous phases was examined under a microscope. The after-flood micrographs are presented in Figure 10. According to the images, NaCl-buffer and LS-6 have similar arrangements between phases in the channels, meaning they have the same effects on the surface wettability. However, LS-3 shows a more hydrophilic situation. It is suggested that a reduced contact angle leads to a higher recovery,[61] translating into lower recovery for oil-wet reservoir rocks (carbonate).[62−64] Although this is true in the case of LS samples, based on the data in this study, the wettability does not seem to be the only defining parameter in the final RF.

3.4.2. Two-step Recovery. To mimic the actual oil recovery processes, crude oil B was displaced first with high salinity brine and then with an LS-3 solution. The average dynamic recovery based on the injected pore volumes is presented in Figure 11. According to the data, high salinity brine reached breakthrough at about 0.6 pore volumes, which was faster than

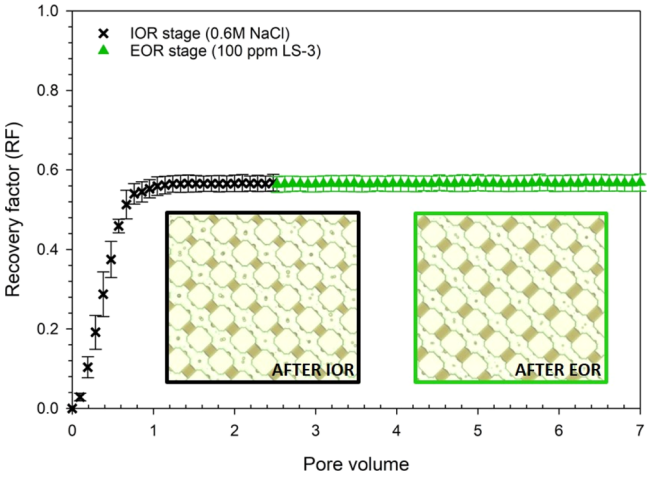

Figure 11. Recovery factor for crude oil B displaced by high salinity brine (IOR part) and LS-3 (100 ppm in NaCl + buffer, EOR part) based on injected pore volumes. Micrographs of oil-flood arrangements after IOR (left) and EOR (right) flood are also presented.

NaCl-buffer solution. In addition, the recovery achieved by high salinity brine showed to be lower than that of the NaCl-buffer solution tested in one-step recovery experiments. High salinity brine reached a plateau at 1.2 pore volume, so the recovery was not changing at the time the EOR flood was introduced to the network. The EOR flood however did not recover any additional oil. Therefore, the recovery efficiency remained the same after it reached steady state during the IOR flood. The small error bars in the image confirm the good repeatability of this experiment. The micrographs of the chip were assessed for changes in wettability. Figure 11 shows the channels after IOR and EOR flood. According to this figure, the EOR flood managed to change the wettability slightly toward water wetness. However, this change must have not been enough to make a change in the recovery factor. Comparing the after-IOR image and the NaCl-buffer image from Figure 10, it is also evident that the NaCl-buffer solution created a slightly more water-wet condition than the high salinity brine.

https://dx.doi.org/10.1021/acsomega.0c04654
ACS Omega XXXX, XXX, XXX−XXX

4. CONCLUSIONS

In this study, the interfacial properties of LS solutions with and without asphaltenes were studied. In addition, applied testing evaluated the suitability of LS for crude oil processing. Here, screening experiments were conducted to test the scenarios emulsion inhibition, produced water treatment, and EOR.

Overall, the following conclusions were drawn:

1. LS are surface-active at the oil/water interface. LSs have a similar surface activity as a classical anionic surfactant such as SDS if they are compared on a molar basis but are less efficient if they are compared at the same mass concentration.
2. LSs were shown to compete with and/or desorb asphaltenes at the oil/water interface.
3. LSs increased the stability of w/o crude oil emulsions if it is used as an inhibitor (solubilized in the aqueous phase) or as a demulsifier (organosoluble complex with a quaternary ammonium).
4. LS had no visible effect on the clarification of o/w emulsions present in produced water.
5. LS flood can, to some extent, alter surface wettability toward water wetness. However, no additional oil recovery was found during an EOR flood.

The results in this study suggested interesting properties, by which LS could replace asphaltenes at the water/oil interface. This destabilizing effect could be exploited, for example, in the processing of crude oil and the treatment of produced water. During applied testing, it became evident, however, that the emulsion stabilization effect dominates over the destabilizing effect. Consequently, we conclude that the studied LS are better suited as an emulsion stabilizer than an emulsion destabilizer.

■ ASSOCIATED CONTENT

Supporting Information

The Supporting Information is available free of charge at https://pubs.acs.org/doi/10.1021/acsomega.0c04654.

Variations of the interfacial tension with sodium dodecylsulfate or lignosulfonate molar concentration at the liquid/liquid interface after 1 h of adsorption; kinetics of adsorption at the liquid/liquid interface of only asphaltenes, only lignosulfonate (LS-4 or LS-6) and mixtures of lignosulfonate (LS-4 or LS-6) and asphaltenes; and evolution of the light transmission for crude oil-in-water emulsions with and without LSs (PDF)

■ AUTHOR INFORMATION

Corresponding Author

Sébastien Simon − *Ugelstad Laboratory, Department of Chemical Engineering, The Norwegian University of Science and Technology (NTNU), N-7491 Trondheim, Norway;* orcid.org/0000-0002-3101-4267; Phone: (+47) 73 59 16 57; Email: sebastien.simon@chemeng.ntnu.no; Fax: (+47) 73 59 40 80

Authors

Marzieh Saadat − *Ugelstad Laboratory, Department of Chemical Engineering, The Norwegian University of Science and Technology (NTNU), N-7491 Trondheim, Norway*

Jost Ruwoldt − *Ugelstad Laboratory, Department of Chemical Engineering, The Norwegian University of Science and Technology (NTNU), N-7491 Trondheim, Norway; RISE PFI AS, 7034 Trondheim, Norway;* orcid.org/0000-0002-0583-224X

Marcin Dudek − *Ugelstad Laboratory, Department of Chemical Engineering, The Norwegian University of Science and Technology (NTNU), N-7491 Trondheim, Norway;* orcid.org/0000-0001-6444-7109

Ross J. Ellis − *Borregaard AS, 1701 Sarpsborg, Norway;* orcid.org/0000-0001-7691-5205

Gisle Øye − *Ugelstad Laboratory, Department of Chemical Engineering, The Norwegian University of Science and Technology (NTNU), N-7491 Trondheim, Norway;* orcid.org/0000-0002-6391-3750

Complete contact information is available at: https://pubs.acs.org/10.1021/acsomega.0c04654

Notes

The authors declare no competing financial interest.

■ ACKNOWLEDGMENTS

This work was carried out as part of the project "Ligno2G: second-generation performance chemicals from lignin" (grant number 269570) funded by the Norwegian Research Council and Borregaard AS.

■ LIST OF SYMBOLS AND ABBREVIATIONS

E^*	complex dynamic apparent dilatational modulus
E'	apparent elastic dilatational modulus
E''	apparent viscous dilatational modulus
EOR	sodium dodecyl sulfate oil recovery
IFT	interfacial tension
IOR	improved oil recovery
$K_{L,A}$	Langmuir equilibrium adsorption constant of component A
LSs	lignosulfonates
MOPS	3-(*N*-morpholino)propanesulfonic acid
MTOAC	methyltrioctylammonium chloride
o/w	oil-in-water emulsion
PW	produced water
QCM	quartz crystal microbalance
R	perfect gas constant
RT	recovery factor
SDS	sodium dodecylsulfate
T	temperature
w/o	water-in-oil emulsion
Γ	surface excess
Γ_m	maximum adsorbed amount (in the Langmuir isotherm)

■ REFERENCES

(1) Vishtal, A.; Kraslawski, A. Challenges in industrial applications of technical lignins. *BioResources* **2011**, *6*, 3547−3568.

(2) Braaten, S. M.; Christensen, B. E.; Fredheim, G. E. Comparison of Molecular Weight and Molecular Weight Distributions of Softwood and Hardwood Lignosulfonates. *J. Wood Chem. Technol.* **2003**, *23*, 197−215.

(3) Aro, T.; Fatehi, P. Production and Application of Lignosulfonates and Sulfonated Lignin. *ChemSusChem* **2017**, *10*, 1861−1877.

(4) Xu, C.; Ferdosian, F. Utilization of Lignosulfonate as Dispersants or Surfactants. In *Conversion of Lignin into Bio-Based Chemicals and Materials*; Springer-Verlag GmbH Germany, 2017; pp 81−90.

(5) Lauten, R. A.; Myrvold, B. O.; Gundersen, S. A. New Developments in the Commercial Utilization of Lignosulfonates. In

Surfactants from Renewable Resources; Kjellin, M., Johansson, I., Eds.; John Wiley & Sons: United Kingdom, 2010.
(6) Lauten, R. A.; Myrvold, B. O.; Gundersen, S. A. New developments in the commercial utilization of lignosulfonates. *Surfactants from Renewable Resources*; Wiley, 2010; 269−283.
(7) Askvik, K. M.; Are Gundersen, S.; Sjöblom, J.; Merta, J.; Stenius, P. Complexation between lignosulfonates and cationic surfactants and its influence on emulsion and foam stability. *Colloids Surf., A* **1999**, *159*, 89−101.
(8) Park, S.; Lee, E. S.; Sulaiman, W. R. W. Adsorption behaviors of surfactants for chemical flooding in enhanced oil recovery. *J. Ind. Eng. Chem.* **2015**, *21*, 1239−1245.
(9) Ruwoldt, J.; PLanque, J.; Øye, G. Lignosulfonate Salt Tolerance and the Effect on Emulsion Stability. *ACS Omega* **2020**, *5*, 15007−15015.
(10) Gundersen, S.; Ese, M.-H.; Sjöblom, J. Langmuir surface and interface films of lignosulfonates and Kraft lignins in the presence of electrolyte and asphaltenes: correlation to emulsion stability. *Colloids Surf., A* **2001**, *182*, 199−218.
(11) Ruwoldt, J.; Simon, S.; Øye, G. Viscoelastic properties of interfacial lignosulfonate films and the effect of added electrolytes. *Colloids Surf., A* **2020**, *606*, 125478.
(12) Gundersen, S. A.; Sjöblom, J. High- and low-molecular-weight lignosulfonates and Kraft lignins as oil/water-emulsion stabilizers studied by means of electrical conductivity. *Colloid Polym. Sci.* **1999**, *277*, 462−468.
(13) Gundersen, S. A. Lignosulfonates and Kraft lignins as oil-in-water emulsion stabilizers. Ph.D. Thesis, University of Bergen, 2000.
(14) Askvik, K. M. Complexation of lignosulfonates with multivalent cations and cationic surfactants, and the impact on emulsion stability. Ph.D. Thesis, University of Bergen, 2000.
(15) Bai, B.; Wu, Y.; Grigg, R. B. Adsorption and Desorption Kinetics and Equilibrium of Calcium Lignosulfonate on Dolomite Porous Media. *J. Phys. Chem. C* **2009**, *113*, 13772−13779.
(16) Bai, B.; Grigg, R. B. Kinetics and Equilibria of Calcium Lignosulfonate Adsorption and Desorption onto Limestone. In *SPE International Symposium on Oilfield Chemistry*; Society of Petroleum Engineers: The Woodlands, Texas, 2005; p 11.
(17) Megiatto, J. D.; Cerrutti, B. M.; Frollini, E. Sodium lignosulfonate as a renewable stabilizing agent for aqueous alumina suspensions. *Int. J. Biol. Macromol.* **2016**, *82*, 927−932.
(18) Qiu, X.; Yan, M.; Yang, D.; Pang, Y.; Deng, Y. Effect of straight-chain alcohols on the physicochemical properties of calcium lignosulfonate. *J. Colloid Interface Sci.* **2009**, *338*, 151−155.
(19) Pang, Y.-X.; Qiu, X.-Q.; Yang, D.-J.; Lou, H.-M. Influence of oxidation, hydroxymethylation and sulfomethylation on the physicochemical properties of calcium lignosulfonate. *Colloids Surf., A* **2008**, *312*, 154−159.
(20) Zulfikar, M. A.; Wahyuningrum, D.; Lestari, S. Adsorption of Lignosulfonate Compound from Aqueous Solution onto Chitosan-Silica Beads. *Sep. Sci. Technol.* **2013**, *48*, 1391−1401.
(21) Qin, Y.; Qiu, X.; Liang, W.; Yang, D. Investigation of Adsorption Characteristics of Sodium Lignosulfonate on the Surface of Disperse Dye Using a Quartz Crystal Microbalance with Dissipation. *Ind. Eng. Chem. Res.* **2015**, *54*, 12313−12319.
(22) Ouyang, X.; Deng, Y.; Qian, Y.; Zhang, P.; Qiu, X. Adsorption Characteristics of Lignosulfonates in Salt-Free and Salt-Added Aqueous Solutions. *Biomacromolecules* **2011**, *12*, 3313−3320.
(23) Deng, Y.; Wu, Y.; Qian, Y.; Ouyang, X.; Yang, D.; Qiu, X. Adsorption and desorption behaviors of lignosulfonate during the self-assembly of multilayers. *BioResources* **2010**, *5*, 1178−1196.
(24) Deng, Y.; Zhang, W.; Wu, Y.; Yu, H.; Qiu, X. Effect of Molecular Weight on the Adsorption Characteristics of Lignosulfonates. *J. Phys. Chem. B* **2011**, *115*, 14866−14873.
(25) Fredheim, G. E.; Christensen, B. E. Polyelectrolyte Complexes: Interactions between Lignosulfonate and Chitosan. *Biomacromolecules* **2003**, *4*, 232−239.
(26) Rana, D.; Neale, G.; Hornof, V. Surface tension of mixed surfactant systems: lignosulfonate and sodium dodecyl sulfate. *Colloid Polym. Sci.* **2002**, *280*, 775−778.
(27) Askvik, K.; Hetlesæther, S.; Sjöblom, J.; Stenius, P. Properties of the lignosulfonate-surfactant complex phase. *Colloids Surf., A* **2001**, *182*, 175−189.
(28) Syahputra, A. E. Experimental Evaluation of Lignosulfonate as a Sacrificial Agent in CO2-Foam Flooding. Doctoral dissertation, New Mexico Institute of Mining and Technology, Department of Petroleum, 1999.
(29) Hong, S. A.; Bae, J. H. Field Experiment of Lignosulfonate Preflushing for Surfactant Adsorption Reduction. *SPE Reservoir Eng.* **1990**, *5*, 467−474.
(30) Hong, S. A.; Bae, J. H.; Lewis, G. R. An Evaluation of Lignosulfonate as a Sacrificial Adsorbate in Surfactant Flooding. *SPE Reservoir Eng.* **1987**, *2*, 17−27.
(31) Novosad, J. Laboratory Evaluation Of Lignosulfonates As Sacrificial Adsorbates In Surfactant Flooding. *J. Can. Pet. Technol.* **1984**, *23*, 6.
(32) Zaki, N. N.; Ahmed, N. S.; Nassar, A. M. Sodium Lignin Sulfonate to Stabilize Heavy Crude Oil-in-Water Emulsions for Pipeline Transportation. *Pet. Sci. Technol.* **2000**, *18*, 1175−1193.
(33) Kelland, M. A. *Production Chemicals for the Oil and Gas Industry*, 2nd ed.; CRC Press, 2014; p 454.
(34) Simon, S.; Nenningsland, A. L.; Herschbach, E.; Sjöblom, J. Extraction of Basic Components from Petroleum Crude Oil. *Energy Fuels* **2010**, *24*, 1043−1050.
(35) Hannisdal, A.; Hemmingsen, P. V.; Sjöblom, J. Group-Type Analysis of Heavy Crude Oils Using Vibrational Spectroscopy in Combination with Multivariate Analysis. *Ind. Eng. Chem. Res.* **2005**, *44*, 1349−1357.
(36) Derkach, S. R.; Krägel, J.; Miller, R. Methods of measuring rheological properties of interfacial layers (Experimental methods of 2D rheology). *Colloid J.* **2009**, *71*, 1−17.
(37) Saadat, M.; Tsai, P. A.; Ho, T.-H.; Øye, G.; Dudek, M. Development of a Microfluidic Method to Study Enhanced Oil Recovery by Low Salinity Water Flooding. *ACS Omega* **2020**, *5*, 17521.
(38) Sinton, D. Energy: the microfluidic frontier. *Lab Chip* **2014**, *14*, 3127−3134.
(39) Lifton, V. A. Microfluidics: an enabling screening technology for enhanced oil recovery (EOR). *Lab Chip* **2016**, *16*, 1777−1796.
(40) Sjöblom, J.; Aske, N.; Harald Auflem, I.; Brandal, Ø.; Erik Havre, T.; Sæther, Ø.; Westvik, A.; Eng Johnsen, E.; Kallevik, H. Our Current Understanding of Water-in-Crude Oil Emulsions.: Recent Characterization Techniques and High Pressure Performance. *Adv. Colloid Interface Sci.* **2003**, *100−102*, 399−473.
(41) Kilpatrick, P. K.; Spiecker, P. M. Asphaltene Emulsions. In *Encyclopedic Handbook of Emulsion Technology*; Sjöblom, J., Ed.; Marcel Dekker, Inc.: New York, 2001; pp 707−730.
(42) Benmekhbi, M.; Simon, S.; Sjöblom, J. Dynamic and Rheological Properties of Span 80 at Liquid-Liquid Interfaces. *J. Dispersion Sci. Technol.* **2014**, *35*, 765−776.
(43) Eastoe, J.; Dalton, J. S. Dynamic surface tension and adsorption mechanisms of surfactants at the air-water interface. *Adv. Colloid Interface Sci.* **2000**, *85*, 103−144.
(44) Bąk, A.; Podgórska, W. Interfacial and surface tensions of toluene/water and air/water systems with nonionic surfactants Tween 20 and Tween 80. *Colloids Surf., A* **2016**, *504*, 414−425.
(45) Santini, E.; Liggieri, L.; Sacca, L.; Clausse, D.; Ravera, F. Interfacial rheology of Span 80 adsorbed layers at paraffin oil-water interface and correlation with the corresponding emulsion properties. *Colloids Surf., A* **2007**, *309*, 270−279.
(46) Lucassen, J.; Van Den Tempel, M. Dynamic measurements of dilational properties of a liquid interface. *Chem. Eng. Sci.* **1972**, *27*, 1283−1291.
(47) Kirby, S. M.; Zhang, X.; Russo, P. S.; Anna, S. L.; Walker, L. M. Formation of a Rigid Hydrophobin Film and Disruption by an

https://dx.doi.org/10.1021/acsomega.0c04654
ACS Omega XXXX, XXX, XXX−XXX

Anionic Surfactant at an Air/Water Interface. *Langmuir* **2016**, *32*, 5542−5551.
(48) Subramanian, S.; Simon, S.; Sjöblom, J. Interfacial dilational rheology properties of films formed at the oil/water interface by reaction between tetrameric acid and calcium ion. *J. Dispersion Sci. Technol.* **2017**, *38*, 1110−1116.
(49) Nenningsland, A. L.; Gao, B.; Simon, S.; Sjöblom, J. Comparative Study of Stabilizing Agents for Water-in-Oil Emulsions. *Energy Fuels* **2011**, *25*, 5746−5754.
(50) Poteau, S.; Argillier, J.-F.; Langevin, D.; Pincet, F.; Perez, E. Influence of pH on Stability and Dynamic Properties of Asphaltenes and Other Amphiphilic Molecules at the Oil−Water Interface†. *Energy Fuels* **2005**, *19*, 1337−1341.
(51) McLean, J. D.; Kilpatrick, P. K. Effects of Asphaltene Solvency on Stability of Water-in-Crude-Oil Emulsions. *J. Colloid Interface Sci.* **1997**, *189*, 242−253.
(52) Hannisdal, A.; Ese, M.-H.; Hemmingsen, P. V.; Sjöblom, J. Particle-stabilized emulsions: Effect of heavy crude oil components pre-adsorbed onto stabilizing solids. *Colloids Surf., A* **2006**, *276*, 45−58.
(53) Schuler, B.; Zhang, Y.; Liu, F.; Pomerantz, A. E.; Andrews, A. B.; Gross, L.; Pauchard, V.; Banerjee, S.; Mullins, O. C. Overview of Asphaltene Nanostructures and Thermodynamic Applications. *Energy Fuels* **2020** DOI: 10.1021/acs.energyfuels.0c00874.
(54) Chang, C.-H.; Franses, E. I. Adsorption dynamics of surfactants at the air/water interface: a critical review of mathematical models, data, and mechanisms. *Colloids Surf., A* **1995**, *100*, 1−45.
(55) Kontturi, A.-K.; Sundholm, G.; Nielsen, K. M.; Zingales, R.; Vikholm, I.; Urso, F.; Weidlein, J.; Zingaro, R. A. The Extraction and Fractionation of Lignosulfonates with Long Chain Aliphatic Amines. *Acta Chem. Scand.* **1986**, *40a*, 121−125.
(56) Buckley, J. S.; Fan, T. Crude Oil/Brine Interfacial Tensions. *Petrophysics* **2007**, *48*, 175−185.
(57) Tang, Q.; Zhou, M.; Yang, D.; Qiu, X. Effects of pH on aggregation behavior of sodium lignosulfonate (NaLS) in concentrated solutions. *J. Polym. Res.* **2015**, *22*, 50.
(58) Dudek, M.; Vik, E. A.; Aanesen, S. V.; Øye, G. Colloid chemistry and experimental techniques for understanding fundamental behaviour of produced water in oil and gas production. *Adv. Colloid Interface Sci.* **2020**, *276*, 102105.
(59) Fakhru'l-Razi, A.; Pendashteh, A.; Abdullah, L. C.; Biak, D. R. A.; Madaeni, S. S.; Abidin, Z. Z. Review of technologies for oil and gas produced water treatment. *J. Hazard. Mater.* **2009**, *170*, 530−551.
(60) Shah, A.; Fishwick, R.; Wood, J.; Leeke, G.; Rigby, S.; Greaves, M. A review of novel techniques for heavy oil and bitumen extraction and upgrading. *Energy Environ. Sci.* **2010**, *3*, 700−714.
(61) Nourani, M.; Tichelkamp, T.; Gaweł, B.; Øye, G. Desorption of crude oil components from silica and aluminosilicate surfaces upon exposure to aqueous low salinity and surfactant solutions. *Fuel* **2016**, *180*, 1−8.
(62) Mohammed, M.; Babadagli, T. Wettability alteration: A comprehensive review of materials/methods and testing the selected ones on heavy-oil containing oil-wet systems. *Adv. Colloid Interface Sci.* **2015**, *220*, 54−77.
(63) Wagner, O. R.; Leach, R. O. Improving Oil Displacement Efficiency by Wettability Adjustment. *Trans. AIME* **1959**, *216*, 65−72.
(64) Morrow, N. R. Wettability and Its Effect on Oil Recovery. *J. Petrol. Technol.* **1990**, *42*, 1476−1484.

https://dx.doi.org/10.1021/acsomega.0c04654
ACS Omega XXXX, XXX, XXX−XXX